

Recognition of road cracks based on multi-scale Retinex fused with wavelet transform

Shenao Liu, Yonghua Han^{*}, Lu Xu

College of Information, Zhejiang Sci-Tech University, Hangzhou, 310018, China

ARTICLE INFO

Keywords:
 Crack recognition
 Multi-scale retinex
 Wavelet transform
 Image enhancement
 Shadow removal
 Bowler-hat transform

ABSTRACT

Cracks are the main diseases of roads and potential threats to road safety. The detection and repair of cracks is the focus of intelligent transportation system research. However, the performance of automatic crack detection is often not good enough due to the uneven illumination, low contrast between the crack and the surrounding pavement and the possible presence of shadows similar in intensity to the crack. In this paper, an improved multi-scale Retinex algorithm is proposed to enhance the crack image. The wavelet transform is integrated into the traditional multi-scale Retinex algorithm to avoid the halo generated by the Retinex algorithm, thereby reducing the image distortion. Meanwhile, the multi-scale Retinex algorithm can make up for the lack of useful information lost by wavelet transform, so the combination of the two can obtain better crack enhancement effect. In addition, the preprocessing of shadow removal is performed before crack enhancement, which effectively eliminates the interference of high-intensity shadows. Through the comparison of objective performance indicators, the newly proposed algorithm can better highlight the crack information. The method proposed in this paper can effectively realize the functions of shadow removal and crack enhancement, so that the recognition accuracy of the overall detection system reaches 95.8%, indicating that the algorithm has high research significance and engineering application value.

Credit author statement

Shenao Liu: Conceptualization, Methodology, Writing original draft.
 Yonghua Han: Writing – original, Funding acquisition. Lu Xu: Validation, Writing – original draft.

1. Introduction

Effective and efficient pavement condition assessment is critical for determining pavement assessment performance and planning repairs. Numerous studies [1–3] have shown that timely and accurate inspection of pavement cracks can help transportation agencies reduce road maintenance costs and extend pavement life. However, the traditional crack detection mainly relies on manual visual inspection, which is time-consuming and labor-intensive in actual operation, and it is difficult to objectively evaluate the degree of road deterioration [4]. Therefore, it is necessary to develop an automatic, accurate and efficient pavement crack detection method. With the development of computer vision and civil engineering image processing, image-based automatic

crack detection technology has gradually replaced the traditional artificial visual detection.

A lot of research has been conducted by scholars in various countries on the problem of pavement crack detection, and the main methods are two major categories [5]: methods based on image characteristics and methods based on machine learning [6]. The methods based on image characteristics can be divided into edge detection, histogram analysis, mathematical morphology, filtering, etc. The machine learning based approaches are further divided into supervised learning and unsupervised learning [7]. From the perspective of development status, the crack recognition technology based on image features is more widely used in the field of engineering [8,9].

Edge detection is a commonly used method to detect pavement cracks. Through common edge detection algorithms [10], such as Sobel [11] and Canny [12], the foreground of the image, i.e. the crack, is extracted. This method can achieve rapid detection, but it needs to manually set many thresholds. The histogram analysis method is to fit a Gaussian curve according to the grayscale histogram of the crack image, and then determine the segmentation threshold according to the fitted

* Corresponding author.

E-mail addresses: liushenao2008@163.com (S. Liu), hanyonghuahan@163.com (Y. Han), xlhit@126.com (L. Xu).

Gaussian curve. It is simple and fast, but the accuracy is low. The method of mathematical morphology [13–15] needs to set the segmentation threshold and the size of the structural element. Although the detection results are better than the above histogram method, this method relies heavily on the selection of the threshold [16]. The difference between the size of the structural element and the selection of the threshold results in different crack segmentation effects. Especially in the case of different crack thicknesses, the segmentation effect will be worse.

From the current state of research in the field of crack recognition, road crack detection often needs to use a threshold-based segmentation method [17,18], but road surface images are often obtained under bad weather and illumination conditions [19,20], and the road damage image data collected due to uneven illumination is quite difficult to use the threshold-based segmentation method to detect the crack edge [21, 22]. In general, the gray value of the crack itself will be lower than the gray value of the non-cracked pavement image, but the opposite may occur in the pavement image collected under the special circumstances of uneven illumination. If the global threshold method is used in the detection, the crack information in the pavement damage image cannot be detected, resulting in the missing or wrong recognition of the crack information in the pavement damage image, which affects the recognition performance. In addition, uneven illumination or insufficient light will lead to another problem, that is, the captured images will have poor contrast, low brightness, blurred local details, sudden changes in brightness, etc., and often accompanied by obvious noise [23]. This makes it difficult for machine vision to extract and analyze information from these images.

Therefore, the collected road damage images must be preprocessed to make necessary preparations for image crack edge detection and automatic recognition, by overcoming the problem of uneven illumination, enhancing the edge information of cracks in road damaged images, and removing interference information that affects subsequent road crack edge recognition. Among many image enhancement algorithms, the Retinex image enhancement algorithm has excellent enhancement effect for problems such as uneven illumination of images. Retinex is a theory of human color vision proposed by Edwin Land [24]. Unlike traditional linear and nonlinear methods that can only enhance a certain type of image features, Retinex can achieve a balance between dynamic range compression, edge enhancement and color constancy. The main core idea of Retinex theory is that most of the object appearance observed by HVS is determined by the reflection ability of the object, and has little relationship with the incident light intensity on the surface of the object [24], so it can well deal with the problem of uneven illumination. Retinex is most commonly used to enhance medical images such as blood vessels and retina. Considering the similarity of texture features between road crack images and medical images, some researchers [25,26] also applied the Retinex image enhancement algorithm to crack image enhancement. Such algorithms The research and development of the crack image enhancement process has greatly improved the effect.

The traditional Retinex algorithm also has defects in image enhancement processing, and the output image has the phenomenon of halo camouflage [27,28], that is, the dark area near the edge is still very dark after image enhancement, which will affect the recognition of subsequent images. In order to solve the shortcomings of Retinex algorithm in image enhancement processing and improve the image enhancement effect, this thesis research proposes an improved image enhancement processing method combining Retinex algorithm and wavelet transform according to the characteristics of Retinex algorithm in image enhancement processing. Through the experimental results, it can be concluded that the improved algorithm in this paper can not only make up for the shortcomings of the traditional Retinex algorithm, but also the processed pictures are clearer and have better visual effects.

2. Shadow removal

The road crack images collected in the natural environment are prone to shadows. The contour of high-intensity shadows is similar to the shape and color of road cracks, which can easily be misjudged as cracks and become one of the main interference factors in crack extraction [29]. The shadow itself is divided into the umbra area and the penumbra area. The umbra area is generally located in the inner area of the shadow. Because all direct light is blocked by the object, the shadow boundary outline will be clearer. The penumbra area is generally located in the edge area of the shadow, the light is partially blocked, the outline of the shadow area is blurred, and the brightness gradually changes from the inside to the outside, showing a smudge effect. In order to eliminate the interference of shadows, this study proposes different shadow removal schemes according to the different characteristics of different shadows. The next two subsections will describe the shadow removal process in detail.

2.1. Shadow removal for umbra areas

The umbra area tends to be the area with the least light intensity in the image, and the light intensity in this area tends to be almost uniform. Shadowed image $\tilde{I}(x, y)$ can be represented as follows:

$$\tilde{I}(x, y) = I(x, y) \cdot C(x, y) \quad (1)$$

where $I(x, y)$ is the shadowless image and $C(x, y)$ is the shadow factor. Therefore, the problem of solving the shadowless image $I(x, y)$ is transformed into the problem of solving the shadow factor $C(x, y)$. The automatic method of solving $C(x, y)$ is described below.

Since the light intensity in the umbra area tends to be almost the same, it can be assumed that the shadow factor $C(x, y)$ is a constant. The most straightforward and simple way to determine c is to find the constant that minimizes the error in the least squares sense. Let P denote the set of pixels in the bright area near the penumbra area, and let S denote the set of pixels in the umbra area close to the penumbra area, the positional relationship of P and S is shown in Fig. 1. We also assume that the sample lengths of P and S are equal. So we have:

$$c = \underset{a}{\operatorname{argmin}} \|P - S + a\|^2 \quad (2)$$

The restoration image I of the original image \tilde{I} in the umbra region can be expressed as:

$$I(x, y) = \tilde{I}(x, y) / c \quad (3)$$

Among them, $\tilde{I}(x, y)$ only represents the original image in the umbra area, which $I(x, y)$ is the image after the restoration of the umbra area.

2.2. Shadow removal for penumbra areas

The shadow removal of the penumbra area is a tough challenge for

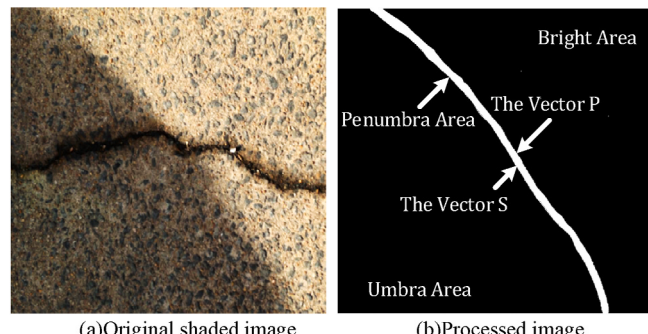


Fig. 1. Schematic diagram of the location of P and S .

multiple causes: one is that the boundary of the penumbra area is relatively blurred and difficult to accurately determine; the other is that the brightness of the penumbra area varies, that is, the shadow factor is not a constant.

Since the shadow factor C in the penumbra area changes at different positions, when calculating the shadow factor $C(x,y)$ of the penumbra area, we take the straight line segment perpendicular to the boundary of the penumbra area, as shown in Fig. 2, and build a model for each straight line segment l_i . Let t_1 and t_2 respectively represent the two boundary points of the penumbra area on the straight line segment, t_1 represent the boundary point between the penumbra area and the light area, t_2 represent the boundary point between penumbra region and shadow region, t_0 be the midpoint of t_1 and t_2 . Let L_{t0} denote the curve consisting of t_0 on all line segments. Similarly, let L_{t1} denote the curve composed of t_1 on all line segments, and L_{t2} denote the curve composed of t_2 on all line segments.

Then, we build the luminance factor model on the line segment l_i :

$$C(t) = \begin{cases} 1, & t < t_1 \\ f(t), & t_1 \leq t \leq t_2 \\ c, & t > t_2 \end{cases} \quad (4)$$

Which c can be calculated in Eq. (2). In order to facilitate the solution, $f(t)$ selects the cubic curve [30]. And $f(t)$ satisfies the following conditions at t_1 and t_2 : $f(t_1) = 1$ and $f(t_2) = c$. The derivative $f'(t)$ of $f(t)$ satisfies: $f'(t_1) = 0$ and $f'(t_2) = 0$, at t_1 and t_2 .

L_{t0} Can be calculated by the following method of minimizing energy, the energy equation is described as follows:

$$E(t_0^{li}) = \sum_{li} \frac{1}{\tilde{I}(t_0^{li})} + \lambda \sum_{li} \sum_{lj \in N(li)} (t_0^{li} - t_0^{lj})^2 \quad (5)$$

where l_i is the first i selected line segment, and N_{li} is the set of line segments adjacent to line segment l_i , the first item of $E(t_0^{li})$ is used to measure the gradient of the image, the second item of $E(t_0^{li})$ is used to measure the smoothness of the curve, and \tilde{I} is the gradient of the image \tilde{I} .

Next, we need to calculate the t_1 and t_2 for each line segment, so that t_0 can be obtained. Once knowing t_0 , we can get an initial curve, that is L_{t0} . Then L_{t0} can be evolved towards the direction of L_{t1} and L_{t2} . Since t_0 is between t_1 and t_2 , L_{t0} should be between L_{t1} and L_{t2} , and L_{t1} and L_{t2} can be seen to have the same shape. For each line segment, we define the energy function:

$$E_{li}(t_1, t_2) = \int_0^{t_1} (\tilde{I} - m_p)^2 dt + \int_{t_2}^{end} (\tilde{I} - m_s)^2 dt + \lambda \int_{t_1}^{t_2} (\tilde{I} - f(t))^2 dt \quad (6)$$

where m_s and m_p are the average values of P and S respectively, $f(t)$ is defined in Eq. (4). In the penumbra region, the problem of brightness variation can be transformed into an energy minimization problem [31]. Then we define the energy functional as follows:

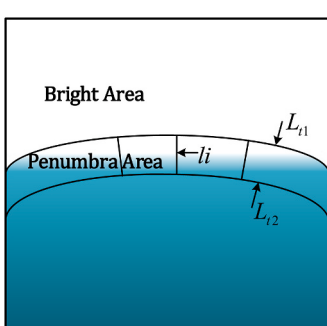


Fig. 2. Schematic of the model of the penumbra region.

$$\tilde{E} = \sum_{li} E_{li}(t_1, t_2) \quad (7)$$

Directly solving the energy functional Eq. (7) is a complicated and time-consuming process. However, as the penumbra region is a very narrow band-shaped region, L_{t0} , L_{t1} and L_{t2} can be approximately regarded as having the same shape [32]. Therefore, when solving L_{t1} , We can pan the whole L_{t0} towards the bright area. Similarly, when solving L_{t2} , the whole L_{t0} can be Panned towards the umbra region. After obtaining $C(t)$, $C(x,y)$ can be obtained. Then the De-shaded image can be calculated by Eq. (8) below:

$$I(x,y) = \tilde{I}(x,y)/C(x,y) \quad (8)$$

Fig. 3 below shows the experimental results of our research on the above shadow removal. From the experimental results, it can be concluded that the algorithm proposed in this study has excellent shadow removal performance and can achieve seamless shadow removal in the umbra/penumbra area. The consistency of illumination intensity between the original shadow and non-shadow areas is maintained, which is not only conducive to subsequent image enhancement, but also eliminates interference for the final crack feature extraction, thereby improving the overall recognition accuracy of the crack detection system.

3. Crack enhancement

As an efficient image enhancement algorithm, Retinex can be basically divided into Single Scale Retinex (SSR) [33,34], Multi Scale Retinex (MSR) [35] and Multi-Scale Retinex with Color Restoration (MSRCR) [36]. The next two subsections will introduce the traditional multi-scale Retinex and the improved multi-scale Retinex algorithm after incorporating wavelet transform in this study in detail.

3.1. Enhancement based on traditional multiscale Retinex

Multi-scale Retinex algorithm is a Retinex algorithm developed from SSR. The multi-scale Retinex is centered on the theory of uniform distribution of incident components. It is believed that the incident component changes slowly in the low frequency band, but in the area with large brightness difference, the incident component changes greatly in the high frequency band. In order to improve the image enhancement effect, multi-scale Retinex expands a Gaussian function $G(x,y)$ with a fixed scale σ_0 in a single-scale Retinex into k Gaussian functions $G_k(x,y)$ with different scales. The general value of k is set to 3, which means that the Gaussian functions G_1 , G_2 , G_3 of three different neighborhood scales of small, medium and large, and the neighborhood scale sizes are described using Gaussian kernel σ_1 , σ_2 , σ_3 . Multiscale Retinex estimates the first k incident image component L_k by convolving the image $I(x,y)$ with the Gaussian function G_k of scale σ_k . The component L_k is expressed as Eq. (9):

$$L_k(x,y) = I(x,y) * G_k(x,y) \quad (9)$$

$$G_k(x,y) = \frac{1}{\sqrt{2\pi}\sigma_k} \exp\left(-\frac{x^2+y^2}{2\sigma_k^2}\right) \quad k = 1, 2, 3$$

The expression of $R(x,y)$ in the logarithmic domain can be obtained by the calculation of the components L_k at different scales and is expressed as:

$$\log(R(x,y)) = \sum_{i=1}^k w_i [\log(I(x,y)) - \log(L_k(x,y))] \quad (10)$$

$$\sum_{i=1}^k w_i = 1$$

where w_i is the weight coefficient, which takes a value of 1/3. By restoring the image from the logarithmic domain to the spatial domain

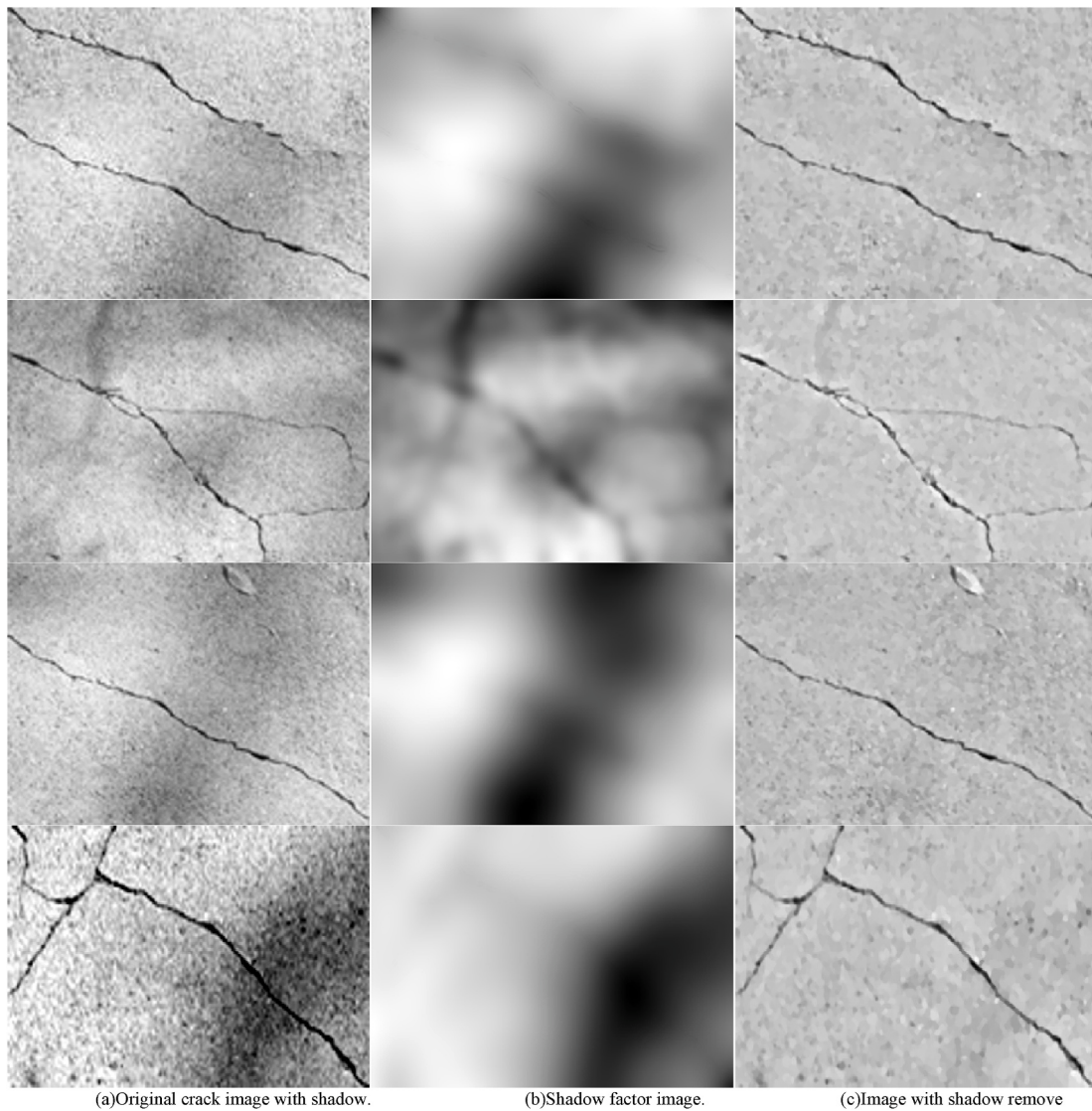


Fig. 3. Experiment results of shadow removal.

to calculate $R(x,y)$, the crack image enhanced by the multi-scale Retinex algorithm can be obtained, which is expressed as:

$$R(x,y) = \frac{I(x,y)}{G_1(x,y)*I(x,y) + G_2(x,y)*I(x,y) + G_3(x,y)*I(x,y)} \quad (11)$$

Compared with the SSR algorithm, the algorithm sets different scale factors for operation on the original basis, which can better highlight the color information while maintaining the dynamic compression range, but the algorithm will amplify the noise when processing low-light images, and it is prone to halo and artifact effect [37].

3.2. Enhancement based on improved multiscale Retinex

As the conventional multi-scale Retinex algorithm is prone to halo during processing, so as to decrease image distortion attributed to the halo phenomenon and obtain better crack enhancement effect, wavelet transform can be combined for image enhancement. The wavelet transform decomposes the image into sub-bands of different frequency bands. According to the scale-space correlation theory, it is known that the noise cannot be transmitted in the scale space. As the number of image decomposition layers increases, it can be considered that the sub-band image contains no noise, but the cost is the loss of useful feature components in the image [38]. The multi-scale Retinex algorithm can

highlight the edge, texture and other details of the image, and can make up for the lack of useful information lost by wavelet transform due to too many decomposition layers. Therefore, this thesis research adopts a multi-scale Retinex algorithm fused with wavelet transform to enhance crack images.

Improved algorithm uses wavelet transform to decompose the image into a low-frequency component and multiple high-frequency components according to the scale parameter [39], and performs different processing on the high and low frequencies respectively. Multi-scale Retinex enhances detailed information in crack images in high frequency image components. The energy contained in the overview information and detail information of the crack is calculated by the image entropy, and ultimately wavelet reconstruction is adopted to acquire the enhanced crack image according to the proportion of each energy to the total energy. Fig. 4 below illustrates the algorithm flow chart:

Owing to the great segmentation accuracy and short average response time of the bowler-hat transform algorithm, this research uses the bowler-hat transform to extract rough crack profile information. It uses disc-shaped structural elements of different diameters and linear structures of different lengths and directions. The elements perform opening operations on the low-frequency image components after wavelet decomposition respectively, and superimpose the maximum difference of the calculation results of the two groups of structural ele-

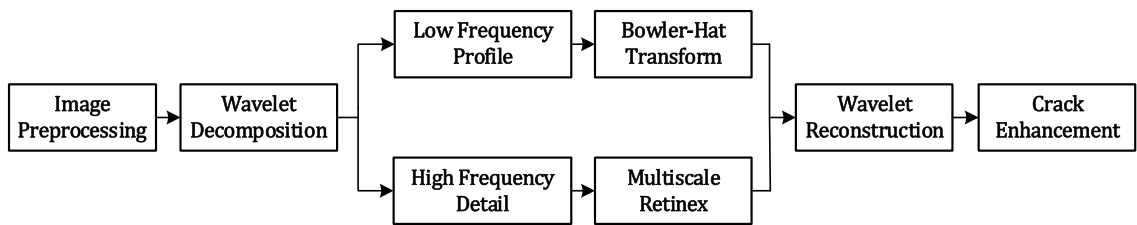


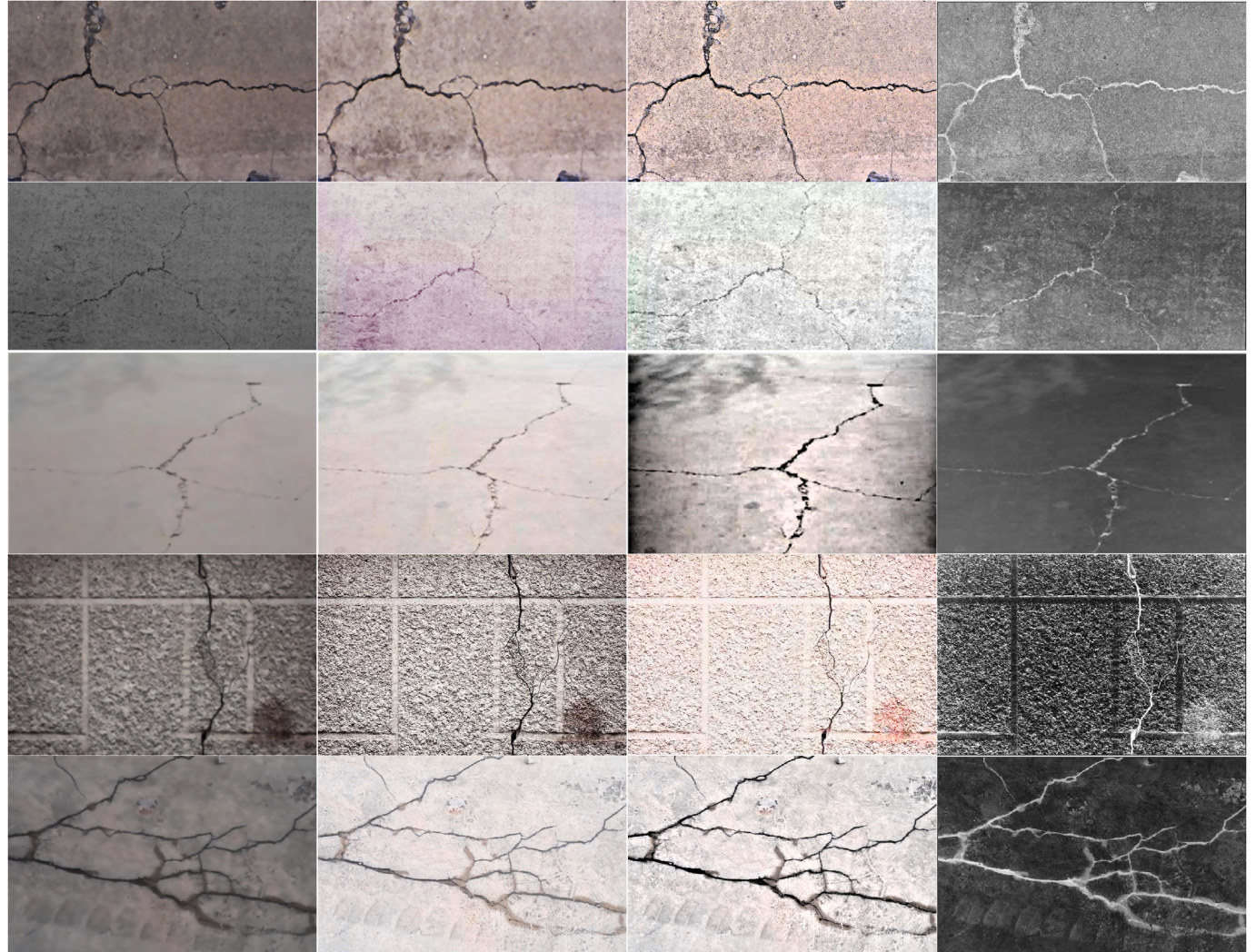
Fig. 4. MSR-Wavelet Transform algorithm flow chart.

ments at different scales as the extracted cracks. The bowler-hat transformation is defined as [40]:

$$I_{bh} = \max_d (|\{I \circ D_d\} - \max_\theta \{I \circ L_{d,\theta}\}|) \quad (12)$$

where I is the low-frequency image after wavelet decomposition, and I_{bh} is the crack image extracted by bowler-hat transform. D is a disc structure operator and L is a linear structure operator. d indicates different scales, $\forall d \in [1, d_{\max}]$, d_{\max} is the largest scale. θ indicates different directions, and $\theta \in [0, 180^\circ]$. θ_{sep} is the step size selected by the angle θ , i.e. θ takes a value every θ_{sep} . Since the crack is a linear structure and expands in any direction, the width is generally 2 to 13 pixels, so d_{\max} is selected

as 13, and the direction interval is θ_{sep} is selected as 10, through the interaction of 18 linear structural elements in directions and 13 disc-shaped structures with different radius, the cracked pixels in the image are matched. For the disc operator, the pixels larger than the scaled are retained as crack pixels, while for the line operator, the pixels along the direction θ and the scale larger than d are retained as crack pixels, and the other pixels are removed as noise points. Image entropy is a vital indicator to determine how much useful information is included in an image. So as to ensure the accuracy of the image after wavelet reconstruction, the image entropy is applied for measuring the energy of the crack information in the image enhanced by the bowler-hat transform and the multiscale Retinex. The calculation formula of image en-



(a) The original crack image. (b) The enhancement results based on the single-scale Retinex algorithm. (c) The enhancement results based on the multi-scale Retinex. (d) The enhancement results based on the improved multi-scale Retinex algorithm proposed in this paper.

Fig. 5. The experimental results of crack enhancement with different algorithms.

tropy is expressed as:

$$H = - \sum_{x=1}^M \sum_{y=1}^N p(x,y) \log p(x,y) \quad (13)$$

Among them, $p(x,y)$ denotes the pixel value of the pixel (x,y) , M and N are the width and height of the image, respectively. Let I_{bh} be the image processed by bowler-hat transformation, and its entropy is H_1 , I_{MSR} is the image after multi-scale Retinex enhancement, and its entropy is H_2 , then the image components that need to be reconstructed are expressed as:

$$I' = \frac{H_1}{H_1 + H_2} I_{bh} + \frac{H_2}{H_1 + H_2} I_{MSR} \quad (14)$$

Image components are reconstructed by inverse wavelet transform, the enhanced crack image can be obtained.

4. Experiments and analysis

For the sake of fully illustrating the enhancement performance superiority of the improved algorithm, the comprehensive image evaluation metrics of the original image, the single-scale Retinex algorithm, the previous multi-scale Retinex algorithm and the enhancement method proposed in this paper are compared. The experimental results of crack images based on the above algorithms are shown in Fig. 5. The experimental results show that when compared with the conventional method, the improved method can better highlight the feature information of cracks, improve the overall visual effect of the image to a large degree, and reduce the phenomenon of halo and artifacts to a certain extent. The processed pictures are clearer, and the image quality has been greatly improved, which is conducive to the subsequent feature recognition of cracks.

So as to objectively compare the crack image enhancement performance of each algorithm, experimental tests were carried out on five image datasets of concrete highway cracks, asphalt highway cracks, rubber runway cracks, bridge cracks, and tunnel cracks. They are compared from the information entropy (reflecting the amount of information in the image, calculated as Eq. (13) above), the brightness mean value (reflecting the overall light and dark effect of the image, calculated as Eq. (15) below), contrast mean value (reflecting the richness of the gray level of the image, calculated as Eq. (16) below), and the time (the time consumed by the image processing process).

Brightness mean value:

$$\text{brightness} = \frac{\sum_{y=1}^N \sum_{x=1}^M g(x,y)}{M \times N} \quad (15)$$

Contrast mean value:

$$\text{contrat} = \sqrt{\frac{\sum_{y=1}^N \sum_{x=1}^M (g(x,y) - \frac{\sum_{y=1}^N \sum_{x=1}^M g(x,y)}{M \times N})^2}{M \times N}} \quad (16)$$

where $g(x,y)$ is the gradient value of the pixel (x,y) , M and N are the width and height of the image, respectively.

The experimental results of the three performance indicators of brightness mean, contrast, and information entropy are shown in Fig. 6, and the image processing time is shown in Table 1. Through the comparison, it can be seen that the images enhanced by traditional single-scale and multi-scale Retinex algorithms in both brightness mean, contrast mean and the information entropy are much stronger than the original images, which verifies the effectiveness of the Retinex algorithm in enhancing the damaged pavement images. However, compared with the algorithm in this study, the performance of the traditional algorithm is significantly worse, which not only reduces the amount of information, but also consumes a longer time. The enhancement algorithm used in this study effectively improves the contrast and distinction between the non-crack area and the crack line in the damaged pavement image, highlights the crack feature information in the image, and achieves the purpose of facilitating crack line extraction. In a comprehensive comparison, the algorithm proposed in this paper still has obvious advantages in the performance of crack image enhancement.

This study finally adopts the traditional multiscale Retinex algorithm and multiscale Retinex fused with wavelet transform algorithm to enhance the image of the crack datasets, and to recognize the crack. To verify the crack image enhancement performance of the improved algorithm and the improvement of the crack recognition accuracy. Part of the crack detection results are shown in Fig. 7, and the crack recognition performance based on the above two algorithms is shown in Table 2.

From the results in Fig. 6 and Table 2, the overall performance of the improved method is higher than that of the previous multi-scale Retinex algorithm. The image processing of enhancement achieves a satisfactory effect, and to a certain extent, it weakens or eliminates the shortcomings of its own algorithm, improves the image's clarity, and improves the efficiency for subsequent image recognition.

Table 1
Image processing time comparison table.

Dataset	SSR Algorithm	MSR Algorithm	Algorithm of this paper
1	6.3584	4.4532	2.6237
2	6.7521	4.9437	2.8625
3	6.3438	4.4390	2.5170
4	5.9682	4.0465	1.9876
5	7.0169	5.1656	2.9725

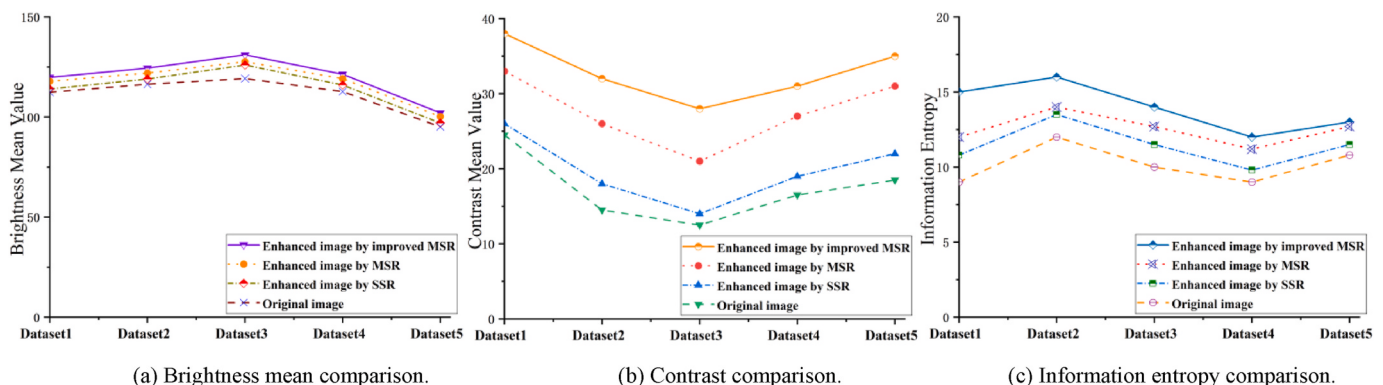
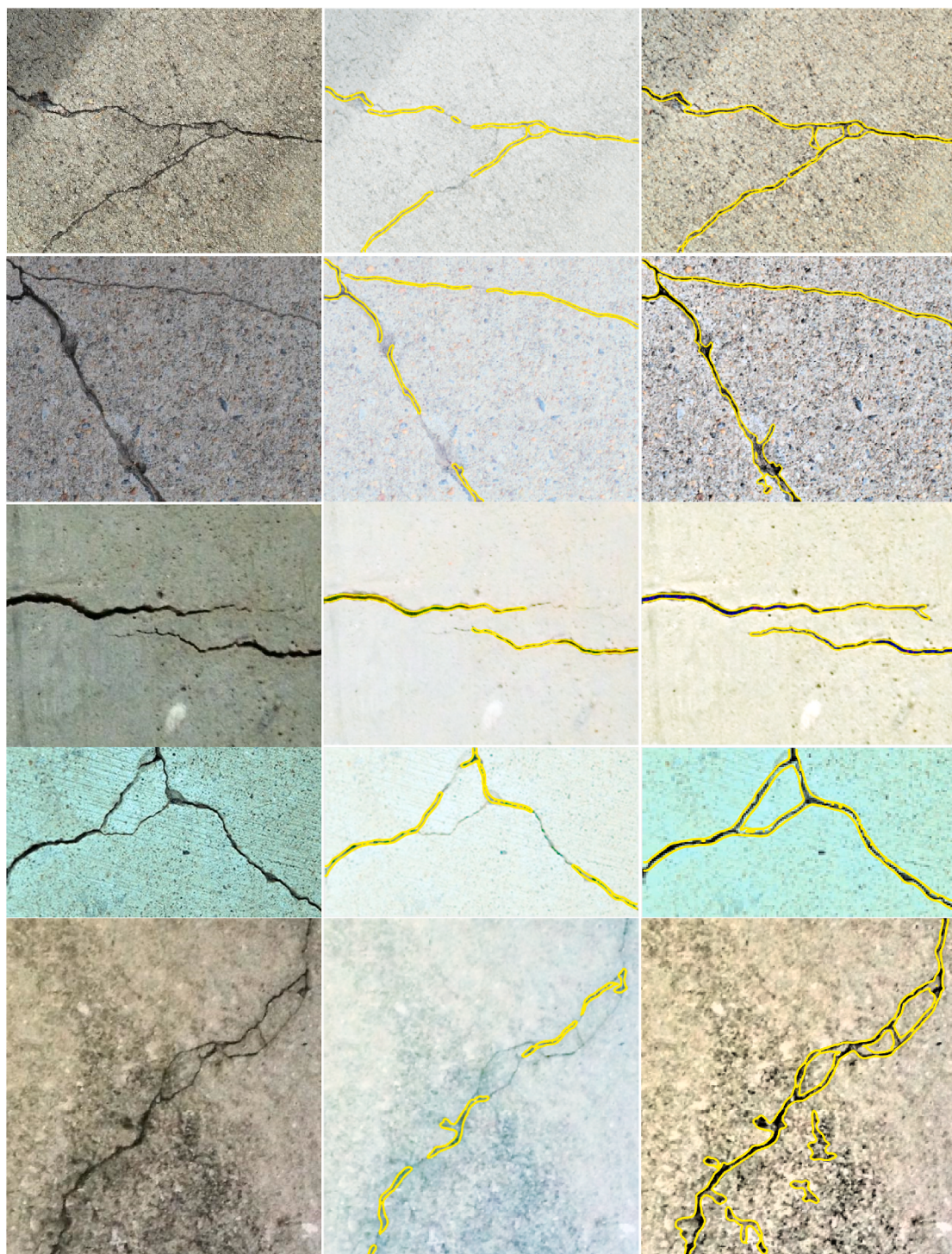


Fig. 6. Comprehensive comparison of enhancement performance based on different algorithms.



(a) the original image. (b) The crack recognition result based on MSR. (c) The crack recognition result based on the algorithm in this paper.

Fig. 7. The experimental results of crack recognition.

Table 2
Recognition performance of crack detection system.

Algorithms	Total number of feature extraction	Total number of feature recognition	Recognition accuracy
Traditional MSR	21,362	16,043	75.1%
The improved MSR	17,452	16,719	95.8%

5. Conclusions

In the road crack detection system based on image processing, the image enhancement processing of pavement damage is of great significance to improve the detection accuracy of crack lines. Therefore, an improved multi-scale Retinex image enhancement algorithm after fusion wavelet transform is proposed in this paper. The algorithm firstly introduces the Retinex algorithm for crack enhancement. Based on the advantage of this algorithm being able to deal with the problem of

uneven illumination of the image, the defect of the original road damaged image illumination in image enhancement is well resolved. At the same time, the wavelet transform is introduced on the basis of the original multi-scale Retinex, which eliminates the halo artifact effect produced by the traditional algorithm, thereby reducing the image distortion. Make up for the shortcomings of the original algorithm. In addition, the removal of shadows in the umbra/penumbra area maintains the consistency of light intensity between shadowed and non-shadowed areas, eliminates the interference caused by high-intensity shadows, and improves the efficiency of subsequent crack enhancement and crack recognition to a certain extent. .

Through the comparison of brightness mean, contrast and information entropy, it can be seen that the newly proposed image enhancement algorithm can perform good preprocessing on the collected road surface damage images. area) and the “low dark” area (crack line), which highlights the characteristic information of cracks in road images and achieves the purpose of extracting crack lines; at the same time, the introduction of bowler-hat transform algorithm makes the average response time shorter, And the segmentation accuracy is improved.

In this study, the above method was applied to the preprocessing step of crack detection. The experimental results verified the effectiveness and feasibility of the algorithm given in this paper. Based on the traditional multi-scale Retinex enhancement algorithm, the recognition accuracy of the crack system was only 75.1%, while The improved enhancement algorithm proposed in this study has improved the accuracy to 95.8%, and its performance is far superior to the traditional method, and the calculation time of each image is relatively short. The experimental results fully demonstrate that the pavement damaged image is enhanced by the new algorithm. extract. Finally, it should be pointed out that improving the time complexity of the improved algorithm proposed in this study has obvious significance to the real-time requirements of the algorithm application in this paper. In summary, this study provides an efficient solution for the preprocessing of road damage images for automatic road crack recognition. At the same time, this method can also be applied to other target detection and recognition systems such as wall cracks and steel plate cracks. Has a wide range of application value.

Funding

This study is supported by the Zhejiang Provincial Natural Science Foundation of China Grant No. LY17F020034.

Declaration of competing interest

We declare that we have no financial and personal relationships with other people or organizations that can inappropriately influence our work, there is no professional or other personal interest of any nature or kind in any product, service and/or company that could be construed as influencing the position presented in, or the review of, the manuscript entitled.

Acknowledgements

None.

References

- [1] Tanaka Y, Fathalla E, Maekawa K. Numerical evaluation of remaining fatigue life of road bridge deck with data assimilation approach. *Bridge Maintenance, Safety, Management, Life-Cycle Sustainability and Innovations*. CRC Press; 2021. p. 1152–60.
- [2] Babashamsi Peyman, et al. Perspective of life-cycle cost analysis and risk assessment for airport pavement in delaying preventive maintenance. *Sustainability* 2022;14(5):2905.
- [3] Evdorides HT, Snaith MS, Anyala M. An analytical study of road pavement fatigue. In: Proceedings of the Institution of Civil Engineers-Transport, vol. 159. Thomas Telford Ltd; 2006. No. 2.
- [4] Mohan Arun, Poobal Sumathi. Crack detection using image processing: a critical review and analysis. *Alex Eng J* 2018;57(2):787–98.
- [5] Hoang Nhat-Duc, Nguyen Quoc-Lam. Automatic recognition of asphalt pavement cracks based on image processing and machine learning approaches: a comparative study on classifier performance. *Math Probl Eng* 2018;2018.
- [6] Feng Xiaoran, et al. Pavement crack detection and segmentation method based on improved deep learning fusion model. *Math Probl Eng* 2020;2020.
- [7] Wang Chunlai, Hou Xiaolin, Liu Yubo. Three-dimensional crack recognition by unsupervised machine learning. *Rock Mech Rock Eng* 2021;54(2):893–903.
- [8] Chen C, et al. Automatic pavement crack detection based on image recognition. In: *International Conference on Smart Infrastructure and Construction 2019 (ICSI)* Driving data-informed decision-making. ICE Publishing; 2019.
- [9] Yun Hae-Bum, Mokhtari Soroush, Wu Liuliu. Crack recognition and segmentation using morphological image-processing techniques for flexible pavements. *Transport Res Rec* 2015;2523(1):115–24.
- [10] Maini Raman, Aggarwal Himanshu. Study and comparison of various image edge detection techniques. *Int J Image Process* 2009;3(1):1–11.
- [11] Yuan Chunlan, et al. Study on image edge detection based on Sobel operator. *Laser Infrared* 2009;39(1):85–7.
- [12] Canby John. A computational approach to edge detection. *IEEE Trans Pattern Anal Mach Intell* 1986;6:679–98.
- [13] Mahler David S, et al. Pavement distress analysis using image processing techniques. *Comput Aided Civ Infrastruct Eng* 1991;6(1):1–14.
- [14] Darwin David, Abou-Zeid Mohamed Nagib, Ketcham Kirk W. Automated crack identification for cement paste. *Cement Concr Res* 1995;25(3):605–16.
- [15] Oliveira Henrique, Correia Paulo Lobato. Automatic road crack segmentation using entropy and image dynamic thresholding. In: *2009 17th European signal Processing Conference*. IEEE; 2009.
- [16] Elbehri H, Hefnawy A, Elewa M. Surface defects detection for ceramic tiles using image processing and morphological techniques. 2005.
- [17] Liu, Yiqing, and Justin KW Yeoh. "Automated crack pattern recognition from images for condition assessment of concrete structures." *Autom Constr* 128 (2021): 103765.
- [18] Qiao Wenting, et al. Research on concrete beam crack recognition algorithm based on block threshold value image processing. *Struct Durab Health Monit* 2020;14(4): 355.
- [19] Hu Yong, Zhao Chun-xia, Wang Hong-nan. Automatic pavement crack detection using texture and shape descriptors. *IETE Tech Rev* 2010;27(5):398–405.
- [20] Qu Zhong, et al. Crack detection of concrete pavement with cross-entropy loss function and improved VGG16 network model. *IEEE Access* 2020;8:54564–73.
- [21] Yu Tiantang, Zhu Aixi, Chen Yingying. Efficient crack detection method for tunnel lining surface cracks based on infrared images. *J Comput Civ Eng* 2017;31(3): 04016067.
- [22] De-Fang Wang, Wei-Ming Zeng, Ni-Zhuan Wang. Road crack detection under uneven illumination using improved k-means algorithm. *Comp Appl Softw* 2015; 32(7):244–7.
- [23] Wang Ping, et al. Low illumination color image enhancement based on Gabor filtering and Retinex theory. *Multimed Tool Appl* 2021;80(12):17705–19.
- [24] Land Edwin H. The retinex theory of color vision. *Sci Am* 1977;237(6):108–29.
- [25] Wang Quanlei, et al. Tunnel lining crack recognition based on improved multiscale retinex and Sobel edge detection. *Math Probl Eng* 2021;2021.
- [26] Qian Bin, Tang Zhenmin, Xu Wei. Pavement crack detection based on improved tensor voting. In: *2014 9th International Conference on Computer Science & Education*. IEEE; 2014.
- [27] Jobson Daniel J, Zia-ur Rahman, Woodell Glenn A. A multiscale retinex for bridging the gap between color images and the human observation of scenes. *IEEE Trans Image Process* 1997;6(7):965–76.
- [28] Hu Yisheng, Zhang Ming. Image contrast enhancement method based on multi-scale wavelet transform[J]. *Mod Electron Technol* 2007;(17):177–8. <https://doi.org/10.16652/j.issn.1004-373x.2007.17.036>.
- [29] Sorincharean Siwaporn, Phiphobmongkol Subskul. Crack detection on asphalt surface image using enhanced grid cell analysis. In: *4th IEEE International Symposium on Electronic Design, Test and Applications (delta 2008)*. IEEE; 2008.
- [30] Chen Jiguo. Shadow segmentation and removal from a single digital image. MS thesis. East China Normal University; 2010.
- [31] Arbel Eli, Hel-Or Hagit. Texture-preserving shadow removal in color images containing curved surfaces. In: *2007 IEEE Conference on Computer Vision and Pattern Recognition*. IEEE; 2007.
- [32] Liu Feng, Gleicher Michael. Texture-consistent shadow removal. In: *European Conference on Computer Vision*. Berlin, Heidelberg: Springer; 2008.
- [33] Wu Lifang, Zhou Peng, Xu Xiao. An illumination invariant face recognition scheme to combining normalized structural descriptor with single scale retinex. In: *Chinese Conference on Biometric Recognition*. Cham: Springer; 2013.
- [34] Tajeripour Farshad, Fekri-Ershad Shervan. Developing a novel approach for stone porosity computing using modified local binary patterns and single scale retinex. *Arabian J Sci Eng* 2014;39(2):875–89.
- [35] Rahman Zia-ur, Jobson Daniel J, Woodell Glenn A. Investigating the relationship between image enhancement and image compression in the context of the multi-scale retinex. *J Vis Commun Image Represent* 2011;22(3):237–50.
- [36] Lin Haoning, Shi Zhenwei. Multi-scale retinex improvement for nighttime image enhancement. *Optik* 2014;125(24):7143–8.
- [37] Meylan Laurence, Sussstrunk Sabine. High dynamic range image rendering with a retinex-based adaptive filter. *IEEE Trans Image Process* 2006;15(9):2820–30.

- [38] Jung Cláudio Rosito, Schacanski J. Adaptive image denoising in scale-space using the wavelet transform. In: Proceedings XIV Brazilian Symposium on Computer Graphics and Image Processing. IEEE; 2001.
- [39] Yang Yi, Su Zhengwei, Sun L. Medical image enhancement algorithm based on wavelet transform. Electron Lett 2010;46(2):120–1.
- [40] Sazak Çigdem, Nelson Carl J, Boguslaw Obara. The multiscale bowler-hat transform for blood vessel enhancement in retinal images. Pattern Recogn 2019;88: 739–50.